The Modelling and Characterization of Dielectric Barrier Discharge-Based Cold Plasma Jets

The Modelling and Characterization of Dielectric Barrier Discharge-Based Cold Plasma Jets

By

G. Divya Deepak, Narendra Kumar Joshi and Ram Prakash

Cambridge Scholars Publishing

The Modelling and Characterization of Dielectric Barrier Discharge-Based Cold Plasma Jets

By G. Divya Deepak, Narendra Kumar Joshi and Ram Prakash

This book first published 2020

Cambridge Scholars Publishing

Lady Stephenson Library, Newcastle upon Tyne, NE6 2PA, UK

British Library Cataloguing in Publication Data
A catalogue record for this book is available from the British Library

ISBN (10): 1-5275-4539-3
ISBN (13): 978-1-5275-4539-7

CONTENTS

List of Figures viii

List of Tables xii

List of Abbreviations xiii

Acknowledgements xv

Preface xvi

Chapter One 1
Introduction
- 1.1 Introduction 1
- 1.2 Plasma 1
- 1.3 Types of Gaseous Discharges 2
  - 1.3.1 Townsend Discharge 3
  - 1.3.2 Glow Discharge 3
  - 1.3.3 Abnormal Glow Discharge 5
  - 1.3.4 ARC Discharge 6
  - 1.3.5 Spark Discharge 6
  - 1.3.6 Corona Discharge 7
- 1.4 Plasma Classification 8
  - 1.4.1 Thermal Plasma 9
  - 1.4.2 Non Equilibrium Cold Plasma 10
- 1.5 Dielectric Barrier Discharges 11
  - 1.5.1 Mechanism of Dielectric Barrier Discharge 13
- 1.6 Classification of Dielectric Barrier Discharge 17
  - 1.6.1 Filamentary Barrier Discharges 17
  - 1.6.2 Multifilament Barrier Discharges 19
  - 1.6.3 Diffuse (Glow) Mode Barrier Discharges 20
- 1.7 Atmospheric Glow Discharge 22

Chapter Two 24
Dielectric Barrier Discharge based Cold Plasma Jets
in Different Configurations
2.1 DBD based Atmospheric Pressure Plasma Jets (APPJ's) 24
2.2 DBD based APPJ's in different Electrode Configurations 24
2.3 DBD like Jets 26
2.4 Applications of DBD Jets 27
2.4.1 Applications of DBD Jets in Textile Industry 29
2.4.2 Applications of DBD Jets in Surface Modification 30
2.4.3 DBD Jets in Pollution Control 33
2.4.4 Applications of DBD Jets in Food Industry 34
2.4.5 Medical Applications of APPJ 37
2.5 Work Done on Modelling of APPJ's 41

Chapter Three 43
Methodology for Analysis of DBD Based Atmospheric
Pressure Plasma Jet
3.1 Governing Equations for Discharge Simulations 44
3.2 Plasma Chemistry 46
3.3 Governing Equations for Flow Simulations 47
3.4 Boundary Conditions 50
3.5 Electrical Characterization of DBD based
Atmospheric Pressure Plasma Jets 50
3.5.1 Effect of the Applied Voltage 52
3.5.2 Effect of the Pulse Frequency 53
3.5.3 Effects of the Gas Flow Rate 54

Chapter Four 55
Modelling and Electrical Characterization of DBD based Atmospheric
Pressure Plasma Jet using Ring Electrode Configuration
4.1 Introduction 56
4.2 Geometry and Experimental Set Up of Ring Electrode
Configuration 57
4.3 Simulation Results 59
4.4 Experimental Results of Argon Plasma Jet using Ring Electrode . 67
4.5 Summary 76

Chapter Five 79
Modelling and Electrical Characterization of Pin Electrode Configuration
5.1 Introduction 80
5.2 Geometry and Experimental Set Up 81

5.3 Modelling of Pin Electrode 83
5.4 Results and Discussion 84
5.4.1 Simulation Results.. 84
5.5 Experimental Results 91
5.6 Summary.. 96

Chapter Six 99
Low Power Miniaturized Atmospheric Pressure Plasma Jet using Floating Helix Configuration
6.1 Introduction.. 99
6.2 Experimental Set Up 101
6.3 Electrical Measurement 104
6.4 Results and Discussion 105
6.4.1 Electrical Characterization of Argon Plasma Jet using Floating Helix and Floating End Ring Electrode.................... 105
6.4.2 Electrical Characterization of Helium Plasma Jet using Floating Helix and Floating End Ring Electrode.................... 110
6.5 Electrical Characterization of Argon and Nitrogen based APPJ using Floating Helix and Floating End Ring Electrode Configuration 114
6.6 Results and Discussion 114
6.6.1 Electrical Characterization of Argon and Nitrogen based APPJ using Floating Helix and Floating End Ring Electrode 114
6.7 Summary.. 121

References 124

LIST OF FIGURES

1.1 V-I characteristics of an electric discharge 3
1.2 Normal glow discharge 4
1.3 Classification of Plasma 8
1.4 Influence of gas pressure on electron temperature and gas temperature (mercury arc plasma) 11
1.5 DBD micro discharges & its equivalent circuit 12
1.6 Electron multiplication and avalanche growth 14
1.7 Avalanche-to-streamer transition and streamer propagation 14
1.8 Micro discharge activity & corresponding Voltage/Charge Lissajous 16
1.9 Lissajous figures of various DBD types. (a) Ozone tube at 1 kHz, (b) CO2 laser at f=50 kHz, (c) plasma display at f=100 kHz voltage (square wave) 16
1.10 Filamentary barrier discharges- process timescale 18
1.11 Multifilaments of a DBD discharge 19

2.1 Schematic of DBD Jet 25
2.2 DBD like Jets 27
2.3 Atmospheric Pressure Plasma Treatment device 29
2.4 SEM Micrographs of UHMPE fibers Top,Control,Middle 1 min He/Air treated, Bottom 2 min He/Air treated 30
2.5 Schematic representation of Nitriding 31
2.6 TEM images of NixFe1-x nano particles synthesized form various combinations of the respective metallocene vapors for Ni and Fe in a continuous flow, atmospheric pressure micro plasma 32
2.7 Experimental set up of micro plasma set up 32
2.8 Schematic diagram of plasma treatment system 34
2.9 Schematic diagram of Floating-Electrode Dielectric Barrier Discharge (FE-DBD) electrode 37
2.10 Experiment setup 38
2.11 Plasma generated inside the root canal of a tooth 39
2.12 Schematic of the plasma jet 39
2.13 Before and after treatment plasma (Tooth cleaning) 40
2.14 (a) Schematic diagram of device. (b) Plasma brush touched by a human finger (5mm is the distance between the blade and the finger) 40

3.1 Experimental of a DBD based Atmospheric Pressure Plasma Jet 51

4.1 Geometry of the double ring electrode 58
4.2 Schematic diagram of double ring electrode configuration with quartz sleeve 58
4.3 Plasma jet generated using ring electrode configuration 59
4.4 Electron density Vs supply frequency at 4.5 kV................................ 60
4.5 Electron density Vs supply frequency at 4.5 kV/25 kHz (With flow) . 61
4.6 Electron density Vs supply frequency at 4.5 kV/25 kHz (static condition).. 61
4.7 Electron temperature Vs supply frequency at 4.5 kV 62
4.8 Electron temperature 3.7 eV at 4.5 kV/25 kHz (static discharge condition).. 62
4.9 Electron temperature at 4.5 kV/25 kHz (Withflow condition)........... 62
4.10 Electric Potential Vs supply Frequency at 4.5 kV 64
4.11 Electrical Potential at 4.5 kV/25 kHz (With flow) 64
4.12 Electrical Potential at 4.5 kV/25 kHz (static condition) 64
4.13 Electron density Vs supply voltage at 25 kHz.................................. 65
4.14 Electron temperature Vs supply voltage at 25 kHz 66
4.15 Electrical potential Vs supply voltage at 25 kHz.............................. 66
4.16 Power consumption in the jet for different frequencies and 3.5 -5.5 kV applied voltage 68
4.17 Oscilloscope current-voltage trace of the cold plasma jet at 5.5 kV/25 kHz.. 69
4.18 Power consumption in the Ar plasma for different voltages and at 10, 15, & 25 kHz applied frequency 69
4.19 Peak discharge current of 176 mA at 5.5 kV/10 kHz 71
4.20 Peak discharge current of 176 mA at 5.5kV, 15 kHz 72
4.21 Oscilloscope current-voltage trace of the cold plasma jet At 6 kV/25 kHz.. 73
4.22 Jet length Vs supply frequency at 4.5 kV 74
4.23 Jet length Vs Supply frequency at 6 kV 74

5.1 Geometry of pin electrode configuration... 82
5.2 Experimental set up of atmospheric pressure plasma jet using pin electrode configuration (with quartz sleeve)...................................... 82
5.3 Cold Plasma jet generated using pin electrode configuration............. 83
5.4 Electron density Vs Supply Frequency at 4.5 kV 85
5.5 Electron density at 4.5 kV/25 kHz (static condition).......................... 86
5.6 Electron density at 4.5 kV/25 kHz (With flow).................................. 86
5.7 Electron temperature Vs Supply Frequency at 4.5 kV........................ 86

5.8 Electron temperature at 4.5 kV/25 kHz (static condition) 87
5.9 Electron temperature at 4.5 kV/25 kHz (With flow) 87
5.10 Electron density Vs Supply voltage at f=25 kHz............................... 88
5.11 Electron temperature Vs Supply voltage at f = 25kHz 89
5.12 Electrical Potential Vs Supply Frequency at 4.5 kV.......................... 90
5.13 Electrical potential reached at 4.5kV/25 kHz (With flow) 91
5.14 Electrical potential reached at 4.5 kV/ 25 kHz (static condition) 91
5.15 Power consumed at 4.5kV/25kHz 92
5.16 Power Vs Supply Frequency at 3.5 & 6.5 kV.................................... 93
5.17 Power consumed 1.06W at 6.5kV/25kHz.. 94
5.18 Power Vs supply voltage at 10 kHz & 25 kHz, 1 lpm....................... 95
5.19 Jet length Vs supply frequency at 4.5kV 96
5.20 Jet length Vs supply frequency at 6.5kV 96

6.1 Experimental set up of floating helix electrode with floating end ring using Argon or Helium gas 102
6.2 Experimental setup of floating helix electrode configuration but without floating end ring using Argon or Helium gas.................... 102
6.3 Experimental setup of floating helix electrode configuration with floating end ring using ($Ar+N_2$) mixture.. 103
6.4 Experimental setup of floating helix electrode configuration but without floating end ring ($Ar+N_2$) mixture 103
6.5 Argon jet generated using floating helix configuration 104
6.6 Helium jet generated using floating helix configuration 104
6.7 Cold plasma jet of (Nitrogen and Argon gases) using floating helix configuration... 105
6.8 Current-voltage (V-I) characteristic of the developed APPJ with floating helix electrode at 2 kV/20 kHz (Argon gas)........................ 106
6.9 Variation of power consumed at different frequencies and at different applied voltages with floating helix electrode 107
6.10 Current-voltage (V-I) characteristic of the developed APPJ with floating helix electrode at 6 kV/25 kHz (Argon gas)......................... 108
6.11 Current-voltage (V-I) characteristic of the developed APPJ with floating helix electrode and end ring configuration at 6 kV/20 kHz 108(Argon gas) 108
6.12 Variation of plasma Jet length at different supply frequencies and different voltages for Argon gas (without end ring) 109
6.13 Variation of plasma Jet length at different supply frequencies and different voltages for Argon gas (with end ring)................................ 110

6.14 Variation of power consumed at different supply voltages and different supply frequencies for floating helix electrode (Helium gas) 111
6.15 Current-voltage (V-I) characteristic of the developed APPJ with floating helix electrode at 6 kV/25 kHz (Helium gas) 111
6.16 Variation of power consumed at different supply voltages and different supply frequencies for floating helix and floating end ring electrodes (Helium gas) 112
6.17 Jet length Vs supply frequency at different voltages (Without end ring) for Helium gas 113
6.18 Jet length Vs supply frequency at different voltages (With end ring) for Helium gas 113
6.19 Current-voltage characteristic of the developed APPJ with floating helix electrode and floating end ring configuration at 7.5 kV/25 kHz ($Ar+N_2$ gas) 115
6.20 Variation of power consumed at different frequencies and at different applied voltages with floating helix electrode 116
6.21 Current-voltage characteristic of the developed APPJ with floating helix electrode and floating end ring configuration at 9.5 kV/25 kHz ($Ar+N_2$ gas) 117
6.22 Variation of plasma Jet length at different supply frequencies and different voltages for $Ar+N_2$ gas (without end ring) 118
6.23 Variation of plasma Jet length at different supply frequencies and different voltages for $Ar+N_2$ gas (with end ring) 119

LIST OF TABLES

1.1 Typical micro discharge parameters in a 1-mm gap in atmospheric-pressure air (Kogelschatz et al.) 15

2.1 Illustration of microbial inactivation results on foods using cold atmospheric pressure plasma 35

3.1 Table of collisions and reactions modelled 46
3.2 Surface reactions of Ar 47

4.1 Electrical characterization of ring electrode 76

6.1 Comparative summary of experimental results using floating helix electrode 120

List of Abbreviations

DBD	Dielectric Barrier Discharge
APPJ	Atmospheric Pressure Plasma Jets
APGD	Atmospheric Pressure Glow Discharge
Hz	Hertz
Q	Total Charge
ε	Relative Permittivity
g	Thickness of Dielectric
d	Discharge Gap
HV	High Voltage Electrode
SEJ	Single Electrode Jets
R	Resistance
C	Capacitance
FEM	Finite Element Method
ρ	Density
$\mathbf{u}$	Velocity Vector
p	Pressure
τ	Viscous Stress Tensor
$\mathbf{F}$	Volume Force Vector
C_p	Specific Heat Capacity at constant pressure

T	Absolute Temperature
q	Heat Flux vector
Q	Heat Source
$\mathbf{m_e}$	Electron Mass
μ_e	Electron Mobility
n_e	Electron Density
n_ε	Electron Energy Density
μ_ε	Electron energy diffusivity
T_e	Electron Temperature
σk	Collison Cross-section
f	Electron Energy Distribution Function
I_{peak}	Peak value of current
Q_{pri}	Primary discharge Current
lpm	Litre per minute
UHMPE	Ultra-high-molecular-weight polyethylene
CVD	Chemical Vapour Deposition
MOCVD	Metal-organic chemical vapour deposition
ICCD	Intensified Charge Coupled Device
mW	Milliwatt
RBD	Resistive Barrier Discharge

ACKNOWLEDGEMENTS

Firstly, I would like to express my sincere gratitude to my guide Prof. N.K Joshi for his continuous support during my Ph.D study and related research, I am also thankful for his patience, motivation and immense knowledge. His keen interest in the subject and critical scientific scrutiny at various stages of research work has enabled me to bring out the book in the present form. I could not have imagined a better advisor and mentor for my Ph.D. study. I am grateful to my co supervisor Dr. Ram Prakash for his immense support, guidance and insightful comments during my research work and also in improving the contents of research work during the writing of papers and this book. I am indebted to Dr. Udit Pal, Mr. Aditya Sinha, and Mr. D.K Pal for their constant help during designing and fabrication of DBD sources and helping me to perform these experiments at CEERI, Pilani MWT Lab.

My heartfelt gratitude to Prof. (Dr) V.K. Jain, Dean, College of Engineering & Technology, Mody University of Science and Technology for his unrelenting support and encouragement throughout my research work. My sincere thanks to Director- CEERI, Pilani who gave me the access to the laboratory and research facilities which made this research work into a reality.

Last but not least. I would like to thank my parents, my wife and my brother for supporting me spiritually throughout writing this book.

PREFACE

Non-equilibrium atmospheric pressure plasma jets (APPJs) are of intense interest in current low-temperature plasma research because of their immense potential for material processing and biomedical applications. The plasma jets generate plasma plumes in open space while providing a significant number of active species, such as radicals, electrons, and ions. Thus, they can be used for direct treatment of materials or living tissues. One of the prerequisites to the biomedical applications is that the plume should be near room temperature and carry a low current under moderate voltage. Depending on the jet configuration and the electrical excitation, the plasma characteristics including heat, charged particle, electric field, and chemically active species may differ significantly. Other important parameters of importance in these studies are the kind of utilized working gas and gas flow rate.

Physically, the breakdown mechanism of APPJs depends strongly on the electron multiplication, which controls the transition from Townsend breakdown to streamer breakdown and finally to glow discharge region. The mobility of charged species in the electric field depend on the gas properties, the gas type determines the electron multiplication and the breakdown mechanism as well as the discharge mode. In addition, different working gases produce different plasma species resulting in different interactions with the targets.

In this research work, the electrical characterization of DBD based APPJ has been done for three electrode arrangements namely, ring electrode, pin electrode and floating helix electrode configurations. In this set of experiments the influence of electrical parameters such as supply voltage and supply frequency on the peak discharge current, power consumed in the plasma and jet length have been analyzed. The results help in optimizing the power consumption in the discharge with longer jet lengths.

From the results of the electrical characterization of these above mentioned electrode configurations, the optimum operating ranges have been established which may help in generation of plasma jet without arcing and without any physical damage to the tube, which could occur due to excessive thermal heat dissipation. The developed cold APPJ of greater lengths may be useful for different biological or other technological applications

Both simulation and experimental results of the developed dielectric barrier discharge based Argon plasma jet in ring electrode configuration shows that the plasma parameters (i.e., electron density, electron temperature, electrical potential) increase with increase in supply frequency and supply voltage under static gas condition and with flow of Argon gas. The values of electron density, electron temperature and electric potential by varying the applied supply voltage and frequency have been calculated using the simulation module and results clearly indicate that discharge is progressing in the glow discharge region (see Fig.4.6, 4.9 & 4.12) for both cases of static discharge condition and with flow of Argon gas. However at all supply frequency and applied voltages, the electron density and electron temperature values are lower under flowing Argon gas conditions due to the lesser availability of electrons compared to the static gas conditions. From our experimental results of ring electrode it is observed at combinations of higher supply voltages and frequency the power consumed reaches a highest value of 1.27 W at 5.5 kV, 25 kHz, with peak discharge current of 144 mA. It is also found from experimental results that for an average power consumption of 0.5W- 0.9 W the tube should be operated between optimum range of 3.5-4.5 kV & 15-20 kHz. It is further observed the power is lost in heating of dielectric material & heating of Argon gas atoms beyond a supply voltage of 5.5 kV irrespective of supply frequency.

Both simulation and experimental results of the developed dielectric barrier discharge based argon plasma jet in pin electrode configuration shows that the plasma parameters (i.e., electron density, electron temperature, electrical potential) increase with increase in frequency and supply voltage for both static condition and with flow of Argon gas. Our experimental results support this fact. It is also observed that at all supply frequencies (10–25 kHz) there is peak consumption of power, occurring for applied voltage between 5.5–6.5 kV. This fact is supported by the increase in peak discharge current value from 232 mA at 5.5 kV to 416 mA at 6.5 kV. Hence at combinations of higher supply voltages and frequency the power consumed reaches a highest value of 1.06 W at 6.5 kV, 25 kHz, which could occur due to multiple streamer formation. As a consequence the supplied power is lost in thermal dissipation of the dielectric tube leading to heating. It is concluded that for this kind of cold plasma jet generation with an average power consumption and peak discharge current value of ~ 0.65 W and 232 mA, the device should be operated between optimum range of 4.5–5.5 kV and 15–25 kHz.

From the comparative analysis of the results of the floating helix and floating end ring electrode experiments with Ar/He/Ar+N_2 gases, it is clearly seen that the maximum power consumed by this helix electrode configuration with end ring is 19 W for (Ar+N_2) mixture as compared to only few mW for Argon or Helium gas (With end ring). This may be attributed to lower breakdown voltage of Ar/He in comparison to molecular gas N_2 which needs higher input energy for dissociation of nitrogen molecule to nitrogen atoms. It has been experimentally observed that for this kind of cold plasma jet (Ar+N_2) generation, average power consumed is~ 6.5 W with peak discharge current value of ~ 1 A. The optimum range of operation of such a device is 7.5–8.5 kV at applied frequency of 15–25 kHz. Since the current is in the range of Ampere so this Ar+N_2 based plasma can be used for surface modification applications and not for biomedical applications as it could damage the living tissue.

Besides the V-I characteristics of these different electrode configurations for DBD based APPJ, jet lengths have been studied as a function of supply voltage, supply frequency and quartz sleeve put at the end of quartz tube. The jet length has been studied for both with sleeve and without sleeve. It has been observed that floating helix electrode configuration operating with helium consumes least power around few mW and may be a potential device for biological applications. The jet generated using mixture of Ar + N_2 shall be rich in excited active species and may be a useful device for surface cleaning and modifications.

The jet length has been studied for both with sleeve and without sleeve for pin electrode and ring electrode. The maximum jet length obtained for ring electrode and pin electrode configurations with quartz sleeve are 29 mm and 26 mm respectively. In floating helix electrode configuration, maximum jet length of 42 mm has been obtained for Helium gas (With end ring) at 6 kV/25 kHz due to penning ionization process in comparison to jet lengths of only 32 mm for Argon gas (With end ring) and jet length of only 26 mm for Ar+N_2 mixture (With end ring) for the same applied conditions.

The presented analysis in this book may help in establishing optimum range of operation for a cold plasma jet without arcing and without any physical damage to the electrodes. Furthermore, experimental results establish the significance of type of working gas on the power consumption as well as on the jet length obtained. These developed cold DBD based APPJ's of larger lengths may be useful to diverse biological applications and surface treatments.

In this research work, a novel electrode design of double floating electrode helix electrode configuration has helped in reducing the power consumption in the range of mW instead of Watts. The jet length has also been enhanced using this novel double floating electrode configuration. The practical applications of the developed floating electrode DBD with longer jet lengths and lower power operations may be realized for the direct plasma treatment on skin and other suitable biomedical applications. The mixed gas APPJ may be useful for surface cleaning and modification and other technological applications.

CHAPTER ONE

INTRODUCTION

1.1 Introduction

The term plasma is used to express a wide variety of macroscopically neutral substances that contain free electrons and ionized atoms or molecules, which demonstrate collective behavior due to long-range coulomb forces. Not all media with charged particles can be termed as plasmas.

1.2 Plasma

Plasma is a state of matter consisting of a mixture of positively- and negatively-charged particles, neutral particles and the excited state of atoms and molecules. Owing to self-generated electric fields plasmas are quasi-neutral, so that the positive and negative charge densities are almost the same, except over a small characteristic length scale (the Debye length). Plasma occurs naturally or can be produced artificially in a laboratory by the application of an electric field to gas and by the process of electron impact, and gas breakdown may occur leading to plasma formation [1, 2]. Plasma is an ionized gas. Ionized implies that at least one electron is free and not bound to an atom or molecule, thus changing the molecules or atoms into positively charged ions. First and foremost, the condition of Debye´s sphere has to be satisfied which determines the quasi-neutrality state. The free electrical charges like electrons and ions make plasma electrically conductive (this electrical conductivity is sometimes greater than that of copper or gold), respond strongly to electromagnetic fields and are very interactive internally. This is because plasma becomes a very intriguing area from both a physical and chemical perspective. As the temperature starts increasing, molecules start to acquire more energy that results in matter transformation. All types of ionized gas should not be termed as plasma (there is inherently some minor degree of ionization in any gas). Ionized gas is frequently termed as plasma once it is electrically neutral in large volume (the electron density is counterbalanced by positive ions) and comprises a large number of the electrically charged particles, necessary to collectively impact its electrical properties and behavior. A source of energy is essential to remove electrons from atoms to create a plasma. Various origins of this energy could be electrical, light (intense visible light from a laser or nuclear fission, ultraviolet light), or thermal. Plasma can be augmented and directed by magnetic and electric fields that permit it to be applied and controlled. Without sufficient sustaining power, the plasma would recombine into neutral gas. Plasma can also be successfully created in laboratories. These technological plasmas are chiefly produced by passing electrical current into a gas. They are divided into two main groups: thermal and non-thermal plasma. As in gas, the plasma temperature is also defined by the average kinetic energy of the charged or neutral particle, atom, or molecule. Hence plasma, as a multicomponent system, possesses the ability to appear at multiple temperatures. In electric discharges that are utilized for plasma generation in the laboratories, energy acquired from the electric field is initially accumulated by electrons between collisions. This energy is then transmitted via other collisions from the electrons to the heavy particles, resulting in the loss of part of their energy. As the electrons are considerably lighter than the heavy particles, they lose only a minor part of their energy (Joule heating). This is essentially the reason that electron temperature in plasma is at the beginning higher than heavy particle temperature [1, 2].

1.3 Types of Gaseous Discharges

The electrical discharges could be performed in various gases with a very extensive range of gas pressure where currents can reach up to 10^6 A. The discharge current may alternate at high/low frequency, with the steady-state having a shorter duration. A typical V-I characteristic of electrical discharge is depicted in Fig. 1.1. The characteristics of discharge can be listed with respect to the appearance and mechanism of ionization as listed below:

(1) Townsend or dark discharge;
(2) Glow discharge;
(3) Abnormal glow discharge; and
(4) Arc discharge.

The spark and corona discharge will also be discussed here.

1.3.1 Townsend Discharge

The Townsend discharge is generally referred to as a non-self-sustained discharge as it is identified by its low current (I <l0^{-6} A). It is an invisible discharge as the excited species density which produces visible light is little. As it is regarded as a discharge which is non-self-sustaining, it needs an external ionizing agent (high temperature/radiation) to create electrons in the gas or from the cathode.

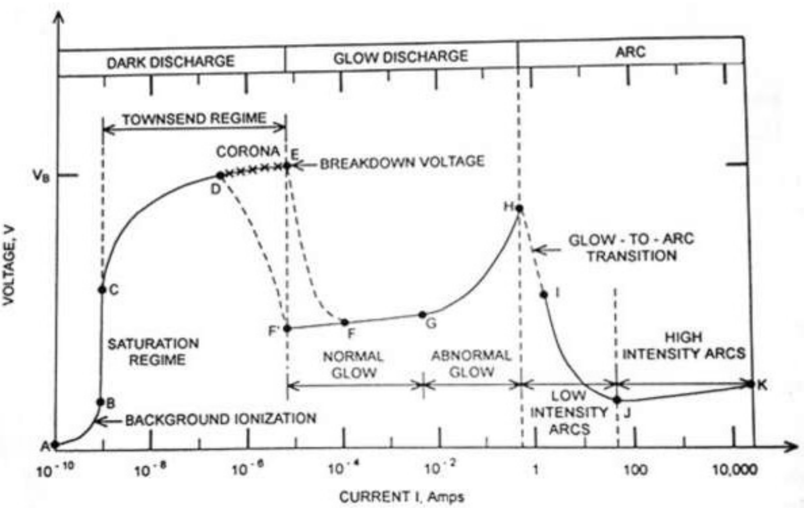

Fig. 1.1 V-I characteristics of an electric discharge [2]

If the Townsend discharge current is increased by an increase in the voltage of supply or by reducing the resistance, the current would rise rapidly by several orders within some time. This point of breakdown relies on the pressure of the gas, the gas type, and the distance between the electrodes. Once breakdown is initiated, the discharge will acquire the appearance of glow/arc-based gas conditions and the circuit.

1.3.2 Glow Discharge

As this type of gas discharge is associated with large brightness which is due to the visible light emitted as a result of excitation collisions of electrons with sufficient energy, hence it is often referred to as glow discharge. Further, the ionization process plays a pivotal role in balancing the loss of ions from a glow discharge in an equilibrium condition with an equivalent gain of the same. Generally, glow discharge is initiated between 2 cold plane metal electrodes in a cylindrically shaped vessel of a few tens of millimeter radius that is filled with gas at a pressure of 0.1-1 mb. The visible light and the 1 mA current, produced from the discharge are spread throughout the tube length as shown in Fig. 1.2 (a). At high pressures >100 mb the cathode glow and the Aston dark space are not seen clearly. When the pressure reduces, the Faraday dark space and the negative glow spread out at the cost of the positive column which could vanish entirely. Glow discharges find their application in lighting devices such as fluorescent lamps, neon lights, and plasma televisions. Detailed examination of this glow with spectroscopy can divulge data about the atomic interactions happening in the gas, thus glow discharges find their application in both analytical chemistry and plasma physics. Glow discharges are also implemented in sputtering (a surface treatment method).

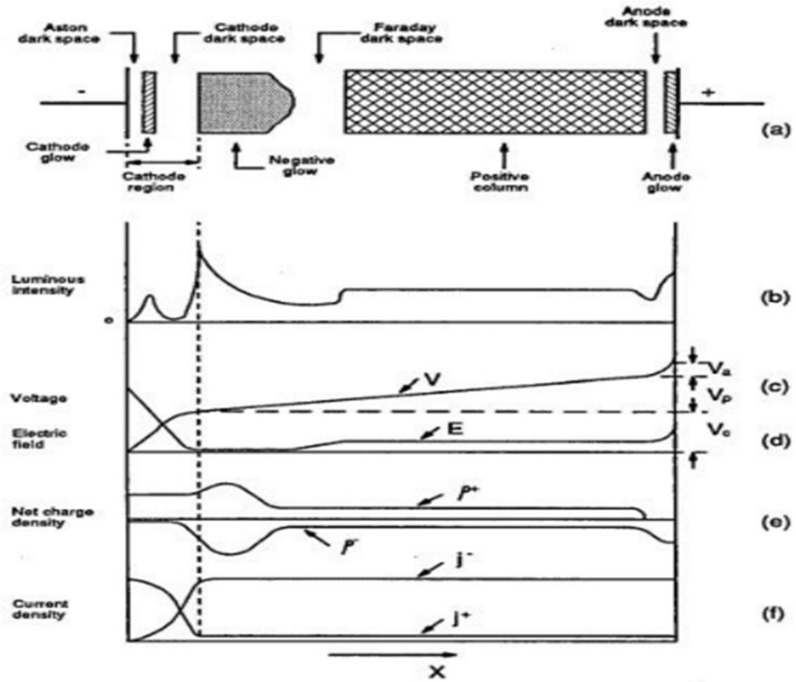

Fig. 1.2 Normal glow discharge [2]

For a gas pressure of more than 0.1 mb, it is observed that the negative regions diminish in the direction of the cathode. For pressure greater than100 mb, only the Faraday dark space is seen visibly. It is observed that the positive column most often occupies the gap that remains, but contraction happens in radial directions at high pressure. If the separation distances in-between the electrodes reduce, then the positive column would reduce in the same proportion without impacting the variation in size of the other zones. The voltage distribution of the glow discharge is depicted in Fig. 1.2(c). The voltage does not change in a linear fashion with the distance from the electrodes as a result of the space-charge effect (Fig. 1.2 (e)). The discharge voltage primarily consists of; V_c = voltage of cathode fall, V_a = anode fall voltage, and V_p = voltage drop in the positive column. The cathode fall voltage is high and varies from 100 V up to 450 V, which signifies that an electric field is high through this region as depicted in Fig. 1.2 (d). The voltage of the positive column changes linearly with respect to its length and hence, the electric field is almost constant along its length. The anode fall voltage is dependent on the gas type and it is the same as the first ionization potential of the gas. The current of this discharge type is primarily electronic instead of being ionic because of the higher mobility that electrons possess. The net charge density and the current density all along the discharge are seen in Figs. 1.2 (e) and (f). The conduction process occurring in a glow discharge and its distribution of the net charge density, emitted light, voltage, and current density have been broadly described. A glow discharge is predominantly generated at low pressure, but it is known that it can be sustained at high pressure up to atmospheric pressure. The discharge in this pressure range is typically referred to as high-pressure glow discharge.

1.3.3 Abnormal Glow Discharge

As the value of current rises in a low-pressure DC electrical discharge tube, then voltage rises gradually near the normal glow region; however, as it goes near point G on the V-I characteristics as shown in Fig. 1.1, voltage increases quickly. This increase happens as the plasma entirely covers the cathode surface. The single way to raise the total current is to let more current flow through the cathode region by raising its voltage, causing a departure away from the Paschen minimum in the region of the cathode. Aside from being extremely luminous, the abnormal glow discharge is very similar to the normal glow discharge, but at times the structures near the cathode combine jointly to give a greater/less uniform luminous intensity all along the complete discharge between the anode and cathode. With the increase of current and voltage, the cathode current density also increases, eventually to a condition where cathode surface heating leads to incandescence. Under the condition of the cathode heating up and being hot enough for the emission of electrons thermionically, discharge will proceed towards the arc regime, provided the power supply has low internal impedance.

1.3.4 Arc Discharge

The three distinctive characteristic features of an arc discharge which are not seen in other forms of discharge are low cathode fall, high luminosity, and relatively high current density. The arc discharge is a self-sustaining discharge, it has a comparatively small cathode potential of nearly 10 V, comparable to the ionization or excitation potential of atoms. This characteristic differentiates the arc discharge from the glow discharge, where the cathode fall is approximately 100 V. The small cathode fall region is resultant of mechanisms of cathode emission that differ from those in the glow discharge. These mechanisms possess the capacity to deliver a larger electron current from the cathode, nearly equal to the total discharge current. This aspect removes the necessity of a significant augmentation of the electron current, whose function is accomplished by the high cathode fall in glow discharges. An arc cathode releases electrons predominantly due to thermionic emission, although some electrons may also be released as field electrons depending on the material of the electrode. The arc discharge is indicated by large currents of 1 to 10^5 A, higher than the current in a glow discharge of 10^{-4} to 10^{-1} A. The cathode current density in arc discharge is considerably greater than that of glow discharges. It may be 100 Amp/cm^2 and can go up to some tens of 10^6 Amp/cm^2. Arc cathodes collect a large amount of energy from the current and attain high temperature, either just locally or over the entire cathode area typically for short intervals of time. The cathode may be affected by vaporization. The emission spectrum of the cathode region in a glow discharge overlaps with the spectrum of the gas which the discharge burns, but on the other hand, the arc spectra depict the lines of vapor of the electrode material. The brightness of the arc column is very high compared to other modes of discharge and is utilized in the illumination field.

1.3.5 Spark Discharge

A spark discharge occurs at a voltage higher than the threshold breakdown level at atmospheric pressure and above. The discharge phenomenon is a swift transitory process such as lightning on a giant scale. Miniature lightning is something like a spark in a laboratory. A streamer progresses at high voltage towards the electrode and forms a conducting pathway between the electrodes. If the current is low, conductivity will decrease. If there is high current it will cause thermal heating of gas, reduce its density and further increase its conductivity. The growth of the current depends on the type of pulse power circuit used. The current can be many orders of magnitude higher than the corona. This kind of discharge is termed the spark discharge. The main dissimilarity between the streamer and the spark is that the plasma of the spark travels towards the thermal plasma, whereas in the streamer channel the gas remains nearly at room temperature. Short discharges produce a spark, which actually stops before they are resolved into arcs. The sparks tend to expand from the high field strength points, i.e. tips. Sparking destroys such tips. If the energy of the sparks is inadequate, the plasma resistivity will surround the tips and the conditioning of the gap is achieved. The violent spark will destroy the high field strength site or even destroy the electrodes [1].

1.3.6 Corona Discharge

When there is a uniform electric field, a steady rise in voltage across a gap results in the breakdown of the gap in the form of a spark without preliminary discharge. However, when the field is non-uniform, a surge in voltage will instantaneously result in a localized discharge in the gas to appear at points with the concentrated electric field intensity. This type of discharge is termed as corona discharge. A corona is a distinctive phenomenon of Townsend dark discharge. The characteristics of corona discharges are faintly luminous, transitory, and audible. A corona discharge happens in the high electric field region near edges and sharp points. Corona discharges are present in numerous forms that are dependent on the electrode's geometrical configurations and polarity of the field. The electrode polarity where the electric field is high indicates two types of corona: the positive corona (the high electric field region is situated around the anode) and the negative corona (the high electric field is focused around the cathode). The ionization in the negative corona is triggered by multiple avalanches which do not arise in the case of the positive corona as the electric field at the cathode is principally too low. It indicates that here the ionization processes are connected to the development of so-called positive streamers. The electric field is sharply non-uniform. The field near one or both electrodes has to be much higher than the rest of the gas. This phenomenon happens close to edges, sharp points or small diameter wires that turn into a low power plasma source. In the corona, the electron temperature is normally about 1 eV and the gas temperature is near to room temperature. These kinds of devices are mainly implemented to provide sufficient adhesion in the treatment of polymer materials.

1.4 Plasma Classification

Plasma is a more or less ionized gas. It is regarded as the fourth state of matter excluding, liquid, solid and gas. In reality, more than 99 per cent of existing matter of the present cosmos is in the plasma state. From a macroscopic viewpoint, plasma is considered to be electrically neutral. Nevertheless, plasma is observed to be conductive electrically and it contains numerous free charge carriers. Two important parameters for the classification of plasma are electron density and electron temperature (see Fig. 1.3). Generally, plasmas are divided into two categories;

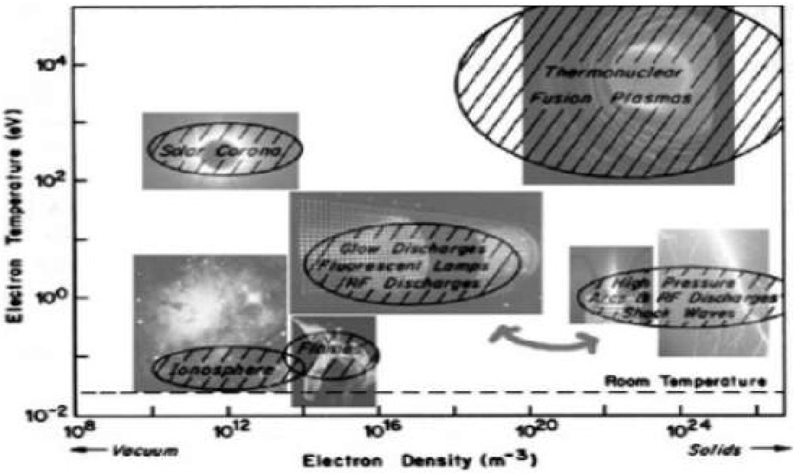

Fig. 1.3 Plasma classification [1]

plasma in thermal equilibrium (thermal plasma) and plasma in non-thermal equilibrium (cold plasma). In thermal plasma, chemical reactions and transitions are dominated by collisions. Furthermore, collision processes are micro-reversible in the case of thermal plasma, indicative of the fact that this collision is balanced by its inverse (kinetic balance, de-excitation or excitation, recombination or ionization). Hence, in thermal plasma, the electron temperature is identical to the gas temperature. Cold plasma is characterized by two temperatures: the temperature of the electron (T_e) and the temperature of the heavy particle (T_h). As there is a large difference in mass among heavy particles and electrons, the temperature of plasma depends on T_h. In cold plasmas, the de-excitation rate of the atom caused by electrons is usually smaller than the radiative de-excitation rate caused by electrons. Consequently, in cold plasma, the density distribution of excited atoms is likely to move away from the Boltzmann distribution, indicating that the temperature of the gas is much less in comparison to the temperature of the electron.

1.4.1 Thermal Plasmas

Plasma comprises molecules/neutral gas atoms, electrons (e) and ions (i). As stated earlier, in thermal plasmas, the gas is basically heated to a high temperature that would partly or fully ionize it. Thus, all the species of gas (electrons, ions, and neutrals) are in thermal equilibrium with one another. In thermal plasma, all its components (ions, electrons, and neutral particles) have a comparable temperature that ranges between 10^3 and 10^4 K. Chemical processes and ionization in those plasmas are estimated by temperature (and indirectly with the help of electric fields using Joule heating). The gas pressure is typically near to atmospheric pressure. A substantial portion of the gas particles is ionized. Plasma processing via atmospheric-pressure plasma has been beneficial in a wide range of applications so far. Atmospheric-pressure plasma has been largely used to increase or activate surface reactions and further it is applied for metal recovery, waste treatment, and welding. Thermal plasma is naturally available, for example, solar plasma. The chief source of thermal plasma made in laboratories is arc discharge. It is produced at high pressure though external circuit resistance is low. This is termed as thermal arc discharge and it is positioned between two electrodes. Thermal arcs generally display high currents and voltages of the order of tens of volts. They yield large amounts of thermal energy at very high temperatures (10,000 K). Arcs are also used alongside gas flow to create high-temperature plasma jets.

Thermal plasmas are widely employed in the processing of materials as they possess high-energy densities and are capable of heating and melting; further, in certain conditions they are also used to vaporize the material to be treated. Thermal plasmas are also increasingly used as a source of reactive species at high temperatures in the plasma chemical synthesis of high-purity materials. The most widely employed plasma-generating device for processing is dc and RF plasma torches. They generate a plasma jet at high temperature in which the material to be processed can be injected for vaporization and melting.

1.4.2 Non-Equilibrium Cold Plasmas

Atmospheric-pressure non-equilibrium cold plasmas have various advantages in comparison to traditional low-pressure static gas discharges. Fig. 1.4 depicts the consequence of gas pressure on the temperature of the electron (T_e) and the temperature of the gas (T_g). It is observed that at a low pressure ranging from 10^{-4} to 10^{-2} kPa, the temperature of the gas is far less in comparison with the temperature of the electron. The heavy particles get ionized or excited during collisions with electrons which are inelastic. These inelastic collisions do not increase the heavy particle temperature. But at higher gas pressure the collisions happening inside the plasma tend to increase. They result in plasma chemistry (occurring as a result of inelastic collisions) and heavy particle heating (as a result of collisions that are elastic in nature). So, the difference between the temperature of electrons and the temperature of gas reduces; the plasma state is near a state of thermal equilibrium. Preventing the heavier particles from getting heated is vital to produce cold plasma at atmospheric pressure. It has already been established that the feeding power density influences the plasma state to a great extent. Specifically, a feeding power low density or a pulsed power supply generates cold plasma at atmospheric pressure [1, 2]. The electron temperature is on the higher side in comparison to the heavy particle temperature. It varies from 10^4 to 10^5 K, whereas ions and neutral constituents, and processed materials are at around a few hundred Kelvins. Chemical processes and ionization in these kinds of plasmas are estimated by electron temperature and also, they are insensitive to the temperature of the gas. Such kinds of plasmas are commonly generated in an extensive range of pressures from a very low value of Pascal to the order of ten atmosphere. The pressure essential for the discharge operation relies on the power supply and the electrode configuration. These plasmas which are weakly ionized can be produced by different kinds of pulsed discharge systems [1].